

# Tartrate Dehydrogenase Catalyzes the Stepwise Oxidative Decarboxylation of D-Malate with both NAD and Thio-NAD<sup>†</sup>

William E. Karsten,<sup>‡</sup> Peter A. Tipton,<sup>§</sup> and Paul F. Cook<sup>\*,‡</sup>

Department of Chemistry and Biochemistry, University of Oklahoma, 620 Parrington Oval, Norman, Oklahoma 73019, and  
Department of Biochemistry, University of Missouri—Columbia, Columbia, Missouri 65211

Received June 11, 2002; Revised Manuscript Received August 6, 2002

**ABSTRACT:** Tartrate dehydrogenase catalyzes the divalent metal ion- and NAD-dependent oxidative decarboxylation of D-malate to yield CO<sub>2</sub>, pyruvate, and NADH. The enzyme also catalyzes the metal ion-dependent oxidation of (+)-tartrate to yield oxalloglycolate and NADH. pH–rate profiles and isotope effects were measured to probe the mechanism of this unique enzyme. Data suggest a general base mechanism with likely general acid catalysis in the oxidative decarboxylation of D-malate. Of interest, the mechanism of oxidative decarboxylation of D-malate is stepwise with NAD<sup>+</sup> or the more oxidizing thio-NAD<sup>+</sup>. The mechanism does not become concerted with the latter as observed for the malic enzyme, which catalyzes the oxidative decarboxylation of L-malate [Karsten, W. E., and Cook, P. F. (1994) *Biochemistry* 33, 2096–2103]. It appears the change in mechanism observed with malic enzyme is specific to its transition state structure and not a generalized trait of metal ion- and NAD(P)-dependent  $\beta$ -hydroxy acid oxidative decarboxylases. The  $V/K_{\text{malate}}$  pH–rate profile decreases at low and high pH and exhibits pK<sub>a</sub> values of about 6.3 and 8.3, while that for  $V/K_{\text{tartrate}}$  (measured from pH 7.5 to pH 9) exhibits a pK<sub>a</sub> of 8.6 on the basic side. A single pK<sub>a</sub> of 6.3 is observed on the acid side of the  $V_{\text{max}}$  pH profile, but the pK<sub>a</sub> seen on the basic side of the  $V/K$  pH profiles is not observed in the  $V_{\text{max}}$  pH profiles. Data suggest the requirement for a general base that accepts a proton from the 2-hydroxyl group of either substrate to facilitate hydride transfer. A second enzymatic group is also required protonated for optimum binding of substrates and may also function as a general acid to donate a proton to the enolpyruvate intermediate to form pyruvate. The <sup>13</sup>C isotope effect, measured on the decarboxylation of D-malate using NAD<sup>+</sup> as the dinucleotide substrate, decreases from a value of 1.0096 ± 0.0006 with D-malate to 1.00787 ± 0.00006 with D-malate-2-*d*, suggesting a stepwise mechanism for the oxidative decarboxylation of D-malate. Using thio-NAD<sup>+</sup> as the dinucleotide substrate the <sup>13</sup>C isotope effects are 1.0034 ± 0.0007 and 1.0027 ± 0.0002 with D-malate and D-malate-2-*d*, respectively.

The tartrate dehydrogenase (TDH)<sup>1</sup> from *Pseudomonas putida* catalyzes three different NAD-dependent reactions (1). The enzyme catalyzes the oxidation of (+)-tartrate to oxalloglycolate, the formation of D-glycerate and CO<sub>2</sub> from meso-tartrate, and the oxidative decarboxylation of D-malate to pyruvate and CO<sub>2</sub>. The dehydrogenase shows the greatest activity in the oxidative decarboxylation reaction of D-malate. All of the reactions catalyzed by TDH require both a divalent

and a monovalent metal ion for activity. The oxidative decarboxylation reaction is enantiomeric to the reaction catalyzed by malic enzyme, with TDH using D-malate and malic enzyme using L-malate.

On the basis of multiple isotope effect studies with NAD as the dinucleotide substrate, the related malic enzyme reaction was shown to be stepwise with respect to its oxidative decarboxylation of L-malate (2, 3). Malic enzyme was also shown to proceed by a general base–general acid mechanism. The general base abstracts a proton from the hydroxyl oxygen of L-malate during the course of the reaction, while the general acid donates a proton to the enolpyruvate formed upon decarboxylation of oxalacetate to yield the final product pyruvate (4, 5). Although the malic enzyme reaction is stepwise with NAD, the reaction is concerted, with hydride transfer and decarboxylation occurring in the same step, when more oxidizing dinucleotide substrates such as APAD or thio-NAD are utilized (6–8). The change in mechanism has been attributed to the oxalacetate intermediate in the reaction existing in a shallow energy well that effectively collapses when the more oxidizing (thermodynamically favorable) dinucleotide substrates are used, leading to the concerted mechanism. The enzyme

<sup>†</sup> This work was supported by grants to P.F.C. from the National Science Foundation (MCB 0091207), a grant from the Oklahoma Center for the Advancement of Science and Technology (HR99-081), and funds for P.F.C. from an endowment to the University of Oklahoma to fund the Grayce B. Kerr Centennial Professorship in Biochemistry.

\* Corresponding author. Tel: 405-325-4581. Fax: 405-325-7182. E-mail: pcook@chemdept.chem.ou.edu.

<sup>‡</sup> University of Oklahoma.

<sup>§</sup> University of Missouri—Columbia.

<sup>1</sup> Abbreviations: APAD, 3-acetylpyridine adenine dinucleotide; Ches, 2-(N-cyclohexylamino)ethanesulfonic acid; Hepes, N-(2-hydroxyethyl)piperazine-N'-2-ethanesulfonic acid; IPMDH, isopropylmalate dehydrogenase; IPTG, isopropyl  $\beta$ -D-thiogalactopyranoside; Mes, 2-(N-morpholino)ethanesulfonic acid; NAD, nicotinamide adenine dinucleotide; NADH, reduced nicotinamide adenine dinucleotide; 6-PGDH, 6-phosphogluconate dehydrogenase; TDH, tartrate dehydrogenase; thio-NAD, thionicotinamide adenine dinucleotide; thio-NADH, reduced thionicotinamide adenine dinucleotide.

6-phosphogluconate dehydrogenase catalyzes the metal ion-independent oxidative decarboxylation of 6-phosphogluconate. Multiple isotope effect studies carried out on 6-PGDH have shown that the reaction proceeds by a stepwise mechanism with both NAD and APAD (9). The absence of a change in mechanism with 6-PGDH suggested that the metal ion may be responsible for destabilizing the oxalacetate intermediate, thus leading to the change in mechanism observed with malic enzyme.

The present studies were carried out to investigate the mechanism of TDH by multiple isotope effect studies to determine if a change in mechanism from stepwise to concerted is a general phenomenon of divalent metal ion-dependent oxidative decarboxylases. In addition, pH studies were carried out to further examine the proposed acid–base mechanism of TDH.

## MATERIALS AND METHODS

**Cell Growth and Purification.** TDH was isolated from *Escherichia coli* cells carrying the plasmid pTDH1 (10) that expresses TDH in the presence of IPTG. The cells were grown in 12 L of LB media at 34 °C with aeration. When the cells reached an OD<sub>600</sub> of 0.5, IPTG was added to a final concentration of 0.5 mM. The culture was allowed to grow an additional 4 h. The cells were harvested by centrifugation at 6000g for 10 min. The harvested cells were suspended in 10 mM potassium phosphate, pH 7, containing 5 mM  $\beta$ -mercaptoethanol (buffer A). The cells were sonicated for 2 min on ice, and the cell debris was removed by centrifugation at 15000g for 20 min. Streptomycin sulfate from an 11% solution was added to the supernatant to bring the final concentration to 1% in the supernatant. After being stirred at 4 °C for 10 min, the solution was centrifuged for 20 min at 15000g. The supernatant was collected, and a heat step was done as previously described (1). The protein solution from the heat step was concentrated by slowly adding solid ammonium sulfate to 80% saturation with stirring at 4 °C. After being stirred for an additional 1 h, the solution was centrifuged for 25 min. The precipitated proteins in the pellet were dissolved in buffer A and dialyzed for 15 h against two 2 L volumes of the same buffer.

The dialyzed enzyme solution was chromatographed on a 3  $\times$  30 cm DEAE-Spherilose column preequilibrated with buffer A using an ISCO liquid chromatography system. The enzyme was eluted with a linear 800 mL potassium phosphate gradient from 10 to 600 mM. The fractions containing TDH activity were combined and precipitated by addition of ammonium sulfate as described above. The precipitated enzyme was dissolved in buffer B consisting of 25 mM Hepes, pH 7, containing 5 mM  $\beta$ -mercaptoethanol and dialyzed for 15 h against two 2 L volumes of the same buffer.

The dialyzed enzyme solution was chromatographed on a 2.5  $\times$  17 cm Blue A–agarose column preequilibrated with buffer B containing 25 mM MgSO<sub>4</sub>. Prior to loading of the enzyme on the column, MgSO<sub>4</sub> was added to the enzyme solution to a concentration of 25 mM. The column was washed with buffer B containing Mg<sup>2+</sup> until the absorbance at 280 nm was near zero. The enzyme was eluted with 500 mM NaCl in the Mg<sup>2+</sup>-containing buffer B. The fractions containing TDH activity were combined and precipitated with

ammonium sulfate as before, and the enzyme was dialyzed for 15 h against 25 mM Hepes, pH 7, 10% glycerol, and 0.5 mM DTT. The enzyme was stored at –20 °C and is >95% pure on the basis of SDS–PAGE.

**Initial Velocity and pH Studies.** Enzyme assays were carried out in 1 mL volumes in 1 cm path-length cuvettes using either an HP-8453 diode array spectrophotometer or a Beckman DU 640 spectrophotometer. Assays were done at 25 °C. Typical assays contained 100 mM K<sup>+</sup>-Hepes, pH 8, 30 mM KCl, 1 mM MnSO<sub>4</sub>, 0.5 mM NAD, and varied concentrations of D-malate or (+)-tartrate. The appearance of NADH was followed at 340 nm ( $\epsilon$  6220 M<sup>–1</sup> cm<sup>–1</sup>). In cases where thio-NAD was used as substrate, the reaction was followed at the absorbance maximum of 395 nm for thio-NADH ( $\epsilon$  11300 M<sup>–1</sup> cm<sup>–1</sup>).

Initial velocity studies as a function of pH studies were carried out essentially as above, except the buffers employed were Mes (pH 6), Hepes (pH 7 and 8), and Ches (pH 9) at the pH indicated and mixtures of the above were used to span the intermediate pH values. Buffers were checked for nonspecific enzyme inhibition, and none was found. The pH of the assay mixtures was determined immediately after completion of the assay. A substrate saturation curve varying either D-malate or (+)-tartrate was obtained at each pH value, maintaining the other substrates and metal ion cofactors at a concentration at least 10 times their respective  $K_m$  or  $K_{act}$  values.

**Primary Deuterium Isotope Effects.** D,L-Malate-2-*d* was prepared according to the method of Tipton (11) by the reduction of oxalacetate with NaB<sup>2</sup>H<sub>4</sub> with one modification. Since it was determined that the L-malate at concentrations at least 10 times those used in determining the primary deuterium isotope effect did not inhibit the TDH reaction, the L-malate-2-*d* formed on reduction of OAA was not removed as done by Tipton (11). The primary deuterium isotope effects were determined by the direct comparison method in assays containing 100 mM Hepes, pH 7.5, 1 mM NAD or thio-NAD, 1 mM MnSO<sub>4</sub>, and 30 mM KCl, with D-malate or D-malate-2-*d* varied from 50 and 500  $\mu$ M with NAD or from 0.2 and 2 mM with thio-NAD.

**<sup>13</sup>C Isotope Effects.** The technique for the determination of <sup>13</sup>C isotope effects is that of O’Leary (12) in which the natural abundance of <sup>13</sup>C in the C-4 position of D-malate-2-*h(d)* is used. Both a 100% and a partial conversion sample are used, and the <sup>12</sup>C/<sup>13</sup>C ratio of the isolated CO<sub>2</sub> from each sample is determined. The relative rates of reaction of <sup>12</sup>C vs <sup>13</sup>C are determined from these ratios and thus the <sup>13</sup>C isotope effect (2). The concentration of D-malate-2-*h(d)* was determined by end-point assay prior to making the reaction mixtures. Reaction mixtures for the low-conversion samples using NAD contained 25 mM Hepes, 0.5 mM DTT, 2 mM MnSO<sub>4</sub>, 10 mM KCl, 10 mM NAD, and 12 mM D-malate-2-*h(d)* in 30 mL. Full conversion samples using NAD contained 25 mM Hepes, 0.5 mM DTT, 2 mM MnSO<sub>4</sub>, 10 mM KCl, 10 mM NAD, and 2 mM D-malate-2-*h(d)* in 30 mL. The partial conversion samples using thio-NAD contained 25 mM Hepes, 0.5 mM DTT, 30 mM KCl, 2 mM MnSO<sub>4</sub>, 7 mM thio-NAD, and 10 mM D-malate-2-*h(d)* in 30 mL. The full conversion samples using thio-NAD contained 25 mM Hepes, 0.5 mM DTT, 30 mM KCl, 2 mM MnSO<sub>4</sub>, 7 mM thio-NAD, and 2 mM D-malate-2-*h(d)* in 30 mL. The pH was adjusted to 6 with KOH, and the reaction

mixtures were sparged with CO<sub>2</sub>-free nitrogen for at least 3 h. The pH was adjusted to pH 8.2 with 1 M KOH, and the mixture was sparged for another 2 h. The reactions were carried out in sealed reaction vessels to prevent contamination with atmospheric CO<sub>2</sub>. The full conversion sample was initiated by the addition of 0.95 mg of TDH in 100  $\mu$ L, and the reaction was allowed to proceed overnight. The full conversion sample was monitored for completeness of reaction by removing an aliquot of the reaction mixture and checking the absorbance at 340 nm. Concentrated sulfuric acid (200  $\mu$ L) was added to the reaction mixture prior to isolation of the CO<sub>2</sub>. The partial conversion samples were initiated by addition of 0.095 mg of TDH in 50  $\mu$ L. Aliquots were removed at time intervals to check reaction progress, and the reaction was quenched by addition of concentrated sulfuric acid (200  $\mu$ L) prior to CO<sub>2</sub> isolation. Isotopic composition of the CO<sub>2</sub> was determined using an isotope ratio mass spectrometer (Finnigan Delta E). All ratios were corrected for <sup>17</sup>O according to Craig (13).

**Oxalacetate Partitioning.** OAA partitioning experiments were carried out following the method of Karsten et al. (7) after the method developed by Grissom and Cleland (14). Partitioning assays were carried out using a HP-8453 diode array spectrophotometer at 25 °C. Typical partitioning reactions contained 100 mM buffer, Mes or Hepes, or a mixture of both, at different pH values. Reactions contained 30 mM KCl, 1 mM MnSO<sub>4</sub>, 0.2 mM NADH(D) or 0.1 mM thio-NADH(D), 1 mM OAA, and 30–50  $\mu$ g of TDH in 1 mL total volumes in 1 cm path-length cuvettes. Concentrations of OAA stock solutions were determined by end-point assay containing 100 mM Hepes, pH 7, 0.2 mM NADH, about 50  $\mu$ M OAA, and 7 units of malate dehydrogenase. An effective extinction coefficient for OAA at 282 nm was determined for each assay. The reaction was allowed to proceed for 5 min to determine background rates at 282 and 340 nm [NADH(D)] or 395 nm [thio-NADH(D)] at which time TDH was added and the reaction monitored simultaneously at 282 and 340 nm or at 395 nm for 5 min. After subtraction of the background rates the partition ratio ( $r_H$ ) expressed as [pyruvate]/[malate] was calculated from

$$d[\text{OAA}]/dt - d[\text{NADH}]/dt = d[\text{pyruvate}]/dt \quad (1)$$

$$(d[\text{pyruvate}]/dt)/(d[\text{NADH}]/dt) = r_H \quad (2)$$

The thio-NADH(D) was prepared in mixtures containing 75 mM Ches/25 mM Hepes, pH 8.4, 30 mM KCl, 0.38 mg of TDH, 1 mM MnSO<sub>4</sub>, 10 mM D-malate-2-*h*(d), and 5 mM thio-NAD in 5 mL volume. The TDH was removed by ultrafiltration, and the protein-free solution was chromatographed on a DEAE-Spherilose column (1.5  $\times$  17 cm) preequilibrated with 25 mM Hepes, pH 8.2. The thio-NADH(D) was eluted with a linear 0–400 mM KCl gradient. Fractions containing the highest concentrations of thio-NADH(D) (typically 1.5–2 mM) were used for the partitioning reactions.

**Data Processing.** Data were fitted using BASIC versions of the Fortran programs developed by Cleland (15). Initial velocity data were fitted using eq 3, data for sequential initial velocity data were fitted using eq 4, and the data for the deuterium isotope effects were fitted using eq 5

$$v = VA/(K_a + A) \quad (3)$$

$$v = VAB/(K_aB + K_bA + AB) \quad (4)$$

$$v = VA/[K(1 + F_iE_{V/K}) + A(1 + F_iE_V)] \quad (5)$$

$$\log y = \log[C/(1 + H/K_1 + K_2/H)] \quad (6)$$

$$\log y = \log[C/(1 + K_2/H)] \quad (7)$$

$$\log y = \log[C/(1 + H/K_1)] \quad (8)$$

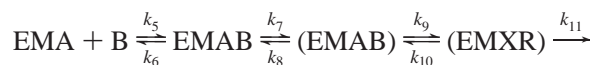
where  $v$  is the initial velocity,  $V$  is the maximum velocity,  $K_a$  and  $K_b$  are the Michaelis constants for  $A$  and  $B$ , respectively,  $A$  and  $B$  are the substrate concentrations,  $F_i$  is the fraction of deuterium in the labeled compound, and  $E_{V/K}$  and  $E_V$  are the isotope effects minus 1 on  $V/K$  and  $V$ , respectively. In eqs 6–8,  $y$  is the parameter of interest,  $C$  is the pH-independent value of  $y$ ,  $H$  is the hydrogen ion concentration, and  $K_1$  and  $K_2$  are the acid dissociation constants for enzyme or substrate functional groups important for binding and/or catalysis. The <sup>13</sup>C isotope effects were calculated using eq 9

$$^{13}(V/K) = \log(1 - f)/\log[1 - f(R_p/R_\infty)] \quad (9)$$

where  $f$  is the fraction of conversion of the reaction and  $R_p$  and  $R_\infty$  are the isotope ratios of the product CO<sub>2</sub> at partial and complete reaction, respectively. The isotope effect nomenclature of Northrop (16) as modified by Cook and Cleland (17) and Hermes et al. (2) is used in this paper.

**Calculation of Intrinsic Isotope Effects and Commitment Factors.** Theory for calculation of intrinsic isotope effects and commitment factors assuming a stepwise mechanism is given in Karsten and Cook (6) for malic enzyme and should apply to TDH under the conditions used to determine the isotope effects. An ordered kinetic mechanism has been reported for TDH with NAD binding prior to D-malate and the divalent metal ion adding in rapid equilibrium prior to D-malate. The kinetic mechanism, with metal ions and dinucleotide substrates at saturating concentration, may be described as in Scheme 1, where  $M$  is Mn<sup>2+</sup>,  $A$  is the oxidized dinucleotide,  $B$  is D-malate,  $X$  is the bound oxalacetate intermediate, and  $R$  is the reduced dinucleotide.

#### Scheme 1



The rate constants  $k_5$  and  $k_6$  are for malate binding and release,  $k_7$  and  $k_8$  represent any precatalytic conformational change leading to a complex poised for catalysis,  $k_9$  and  $k_{10}$  are for forward and reverse hydride transfer steps, and  $k_{11}$  represents the decarboxylation step. The affinity of the enzyme for CO<sub>2</sub> is low; a concentration of 100 mM HCO<sub>3</sub><sup>−</sup> is required to see any inhibition at all (1); consequently, the release of CO<sub>2</sub> is likely fast, making decarboxylation irreversible. The equations for the isotope effects are

$$^D(V/K) = [^Dk_9 + c_f + ^DK_{eq}(c_r)]/[1 + c_f + c_r] \quad (10)$$

$$^T(V/K) = [^Dk_9^{1.44} + c_f + (^DK_{eq})^{1.44}(c_r)]/[1 + c_f + c_r] \quad (11)$$



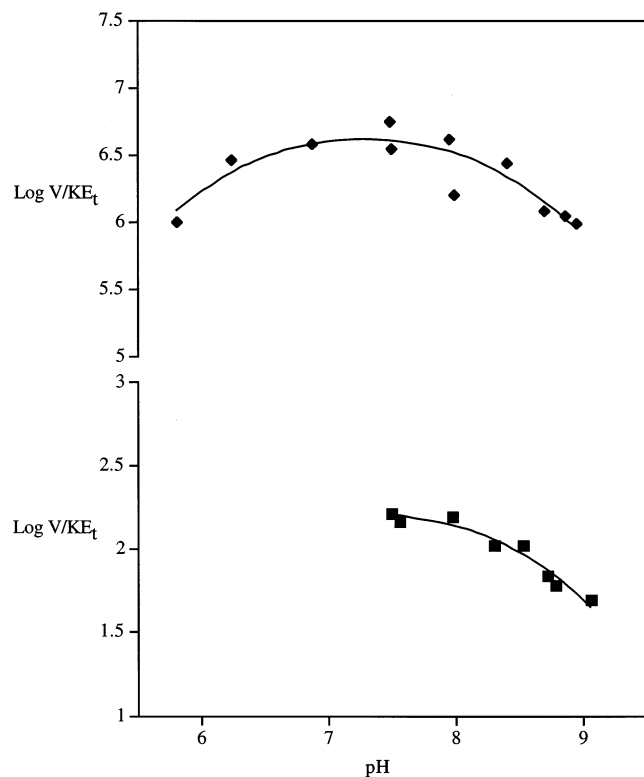


FIGURE 1: pH dependence of  $V/K_{\text{malate}}$  (◆) and  $V/K_{\text{tartrate}}$  (■) for TDH. The points are the experimental data, and the curves are derived from a fit of the data using eq 6 for  $V/K_{\text{malate}}$  and eq 7 for  $V/K_{\text{tartrate}}$ .

$$^{13}(V/K) = [^{13}k_{11} + (1 + c_f)/c_r]/[1 + (1 + c_f)/c_r] \quad (12)$$

$$^{13}(V/K)_D = [^{13}k_{11} + ({}^Dk_9/{}^D K_{\text{eq}}(c_r))(1 + c_f/{}^Dk_9)]/[1 + ({}^Dk_9/{}^D K_{\text{eq}}(c_r))(1 + c_f/{}^Dk_9)] \quad (13)$$

$$r_H = (1 + c_f)/c_r \quad (14)$$

$$r_D = (k_{11}/k_{10})({}^Dk_9 + c_f)/{}^D K_{\text{eq}} \quad (15)$$

where the forward commitment to catalysis is  $c_f = (k_9/k_8)(1 + k_7/k_6)$ , the reverse commitment to catalysis is  $c_r = k_{10}/k_{11}$ ,  ${}^Dk_9$  is the intrinsic primary deuterium isotope effect,  $^{13}k_{11}$  is the intrinsic primary  $^{13}\text{C}$  isotope effect,  $r_H$  is the partition ratio for the OAA intermediate,  $r_D$  is the partition ratio determined with NADD, and  ${}^D K_{\text{eq}}$  is the deuterium isotope effect on the equilibrium constant [determined by Cook et al. (18) to be 1.18]. The commitment factors and intrinsic isotope effects were calculated as described in Karsten and Cook (6).

## RESULTS

**Initial Velocity Studies and pH Dependence of the TDH Reaction.** Initial velocity data using D-malate and thio-NAD as the varied substrates were fitted using eq 2 and yielded the following values for the kinetic parameters:  $K_{\text{malate}} = 0.5 \pm 0.1$  mM,  $K_{\text{thio-NAD}} = 0.11 \pm 0.03$ ,  $V/K_{\text{malate}}E_t = 1.86 \times 10^4 \text{ M}^{-1} \text{ s}^{-1}$ ,  $V/K_{\text{thio-NAD}}E_t = 9.3 \times 10^4 \text{ M}^{-1} \text{ s}^{-1}$ , and  $V/E_t = 9.3 \text{ s}^{-1}$ .

The pH dependence of the TDH reaction with either D-malate or (+)-tartrate as the varied substrate is shown in Figure 1. The  $V/K_{\text{malate}}$  pH profile decreases to limiting slopes

Table 1: Summary of  $\text{p}K_a$  Values Estimated for TDH-Catalyzed Reactions

parameter	pH-independent value	$\text{p}K_1$	$\text{p}K_2$
$V/K_{\text{D-malate}}E_t$	$8.3 \times 10^4 \text{ M}^{-1} \text{ s}^{-1}$	$6.3 \pm 0.2$	$8.3 \pm 0.2$
$V_{\text{D-malate}}/E_t$	$9.3 \text{ s}^{-1}$	$6.3 \pm 0.2$	
$V/K_{\text{tartrate}}E_t$	$1.7 \times 10^2 \text{ M}^{-1} \text{ s}^{-1}$	ND <sup>a</sup>	$8.62 \pm 0.05$
$V_{\text{tartrate}}/E_t$	$0.56 \text{ s}^{-1}$	ND <sup>a</sup>	

<sup>a</sup> Not determined in the present work. Tipton and Peisach (1) reported a  $\text{p}K_a$  value of about 6.5 on  $V/K_{\text{tartrate}}$  and 6.6 on  $V_{\text{tartrate}}$ .

Table 2: Isotope Effects for TDH with NAD or Thio-NAD as the Dinucleotide Substrate

sub- strate	${}^D(V/K)$	${}^D V$	$^{13}(V/K)_H$	$^{13}(V/K)_D$
NAD	$1.46 \pm 0.14$ (5) <sup>a</sup>	$1.09 \pm 0.09$ (5)	$1.0096 \pm 0.0006$ (2)	$1.00787 \pm 0.00006$ (3)
thio- NAD	$1.51 \pm 0.11$ (4)	$1.4 \pm 0.4$ (4)	$1.0034 \pm 0.0007^b$ (3)	$1.0027 \pm 0.0002$ (3)

<sup>a</sup> The values in parentheses are the number of replicate determinations done, and the standard errors reported are on the average of the replicates. <sup>b</sup> One additional individual determination of the  $^{13}\text{C}$  isotope effect was made for both  $^{13}(V/K)_H$  and  $^{13}(V/K)_D$ ; however, inclusion of these values, 1.0065 and 0.9976, respectively, resulted in average values of  $1.0042 \pm 0.0017$  for  $^{13}(V/K)_H$  and  $1.0015 \pm 0.0025$  for  $^{13}(V/K)_D$ . Using these average values for the  $^{13}\text{C}$  isotope effects results in a calculated value for  ${}^D(V/K)$  of 3.3 using the equation  $(^{13}(V/K)_H - 1)/(^{13}(V/K)_D - 1) = {}^D(V/K)/{}^D K_{\text{eq}}$  (see text), which is quite dissimilar to the experimentally determined value of 1.51 for  ${}^D(V/K)$ . Since these two values for the isotope effects are quite different from the average and inclusion leads to a calculated value of  ${}^D(V/K)$  considerably different from the experimentally determined value, the determination of these two values was thought to be in error for an unknown reason and was consequently not included in calculating the values reported in the table.

of +1 and -1 at low and high pH, respectively, giving calculated  $\text{p}K_a$  values of about 6.3 and 8.3. The  $V/K_{\text{tartrate}}$  pH profile decreases at high pH with a limiting slope of -1, giving an estimated  $\text{p}K_a$  of about 8.6. A  $\text{p}K_a$  of about 6.3 is estimated from the  $V_{\text{malate}}$  pH profile, Figure 2, similar to the  $\text{p}K_a$  on the acid side of the  $V/K_{\text{malate}}$  pH profile. The  $\text{p}K_a$  observed on the basic side of the D-malate and tartrate  $V/K$  profiles is not observed in either of the  $V$  profiles. The  $\text{p}K_a$  values and pH-independent values of the kinetic parameters are summarized in Table 1.

**Isotope Effects.** The primary deuterium and  $^{13}\text{C}$  isotope effects are summarized in Table 2. The primary deuterium isotope effect on  $V/K$  with NAD as the dinucleotide substrate is 1.46 and is within error identical to the value reported previously (11). The primary deuterium isotope effect is nearly the same (1.51) when thio-NAD is the dinucleotide substrate. The  $^{13}\text{C}$  isotope effects are small with either NAD or thio-NAD and decrease in both cases upon deuteration of D-malate. Using eqs 8–12, the data for the isotope effects, partition ratios (see below), and the value of 2.08 for  ${}^T(V/K)$  from Tipton (11), estimates of the intrinsic deuterium isotope effect and commitment factors may be calculated with NAD as the dinucleotide substrate. The values are  ${}^Dk = 7.8$ ,  $c_f = 5.2$ ,  $c_r = 14.5$ , and  $^{13}k = 1.014$ .

**Partitioning of Oxalacetate.** Partitioning of oxalacetate was found to be pH dependent as shown in Figure 3. The pyruvate/malate partition ratios and the  $\text{p}K_a$  values, determined from a fit of the partitioning data using eq 5, are summarized in Table 3. The partition ratios increase on deuteration of the dinucleotide substrate and are considerably

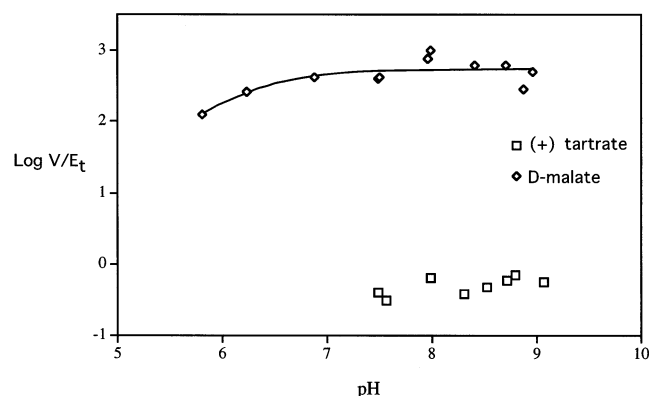


FIGURE 2: pH dependence of  $V_{\text{malate}}$  and  $V_{\text{tartrate}}$  for TDH. The points are the experimental data, and the curve is derived from a fit of the data using eq 8 for  $V_{\text{malate}}$ .

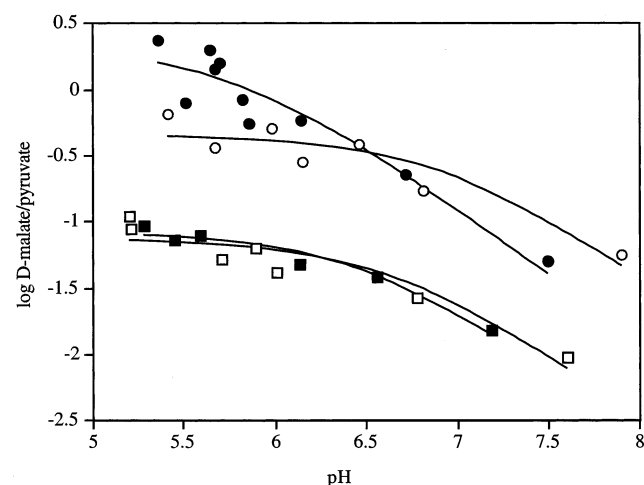


FIGURE 3: pH dependence of the malate/pyruvate partition ratio with NADH (●), NADD (○), thio-NADH (■), and thio-NADD (□). The points are the experimental data, and the curves are derived from a fit of the data using eq 7.

Table 3: pH Dependence of the Pyruvate/Malate Partition Ratios for the Oxalacetate Intermediate in the TDH-Catalyzed Oxidative Decarboxylation Reaction

dinucleotide	partition ratios <sup>a</sup>	$r_{\text{H}}/r_{\text{D}}$	$\text{pK}_{\text{a}}$
	$r_{\text{H}}$ or $r_{\text{D}}$		
NADH	$0.45 \pm 0.16$	0.2	$5.7 \pm 0.3$
NADD	$2.2 \pm 0.4$		$7.0 \pm 0.2$
thio-NADH	$9 \pm 1$	0.75	$6.5 \pm 0.1$
thio-NADD	$12 \pm 1$		$6.5 \pm 0.1$

<sup>a</sup> The partition ratios are the pH-independent values calculated from a fit of the data using eq 5. The partition ratio is defined as the ratio of the net rate constants for formation and release of pyruvate to formation and release of malate beginning with the E–NADH–Mg–oxalacetate complex.

greater with thio-NADH(D) than with NADH(D). The  $\text{pK}_{\text{a}}$  values on the partition ratios range from about 5.7 to 7.0 with an average value around 6.5.

## DISCUSSION

**Interpretation of the pH–Rate Profiles.** The pH studies of Tipton and Peisach (1) were extended in the current work to include a higher pH range and revealed a second  $\text{pK}_{\text{a}}$  value for an enzymatic group that must be protonated for optimum activity at limiting reactant concentration. The  $\text{pK}_{\text{a}}$  on the

acid side of the  $V/K$  profiles is similar to the  $\text{pK}_{\text{a}}$  of about 6.7 reported earlier for  $V/K_{\text{malate}}$  and to the value of 6.5 reported for the  $V/K_{\text{tartrate}}$  pH–rate profiles (1). The  $\text{pK}_{\text{a}}$  on the acid side of the profiles is likely an enzymatic group required to be unprotonated for activity which accepts the proton from the 2-hydroxyl group of D-malate or (+)-tartrate to facilitate hydride transfer as suggested previously (1). For the oxidative decarboxylation reaction catalyzed by TDH, in a stepwise mechanism (see below) where hydride transfer precedes decarboxylation, an oxalacetate intermediate will be formed. Decarboxylation of the oxalacetate intermediate will initially result in the formation of enolpyruvate. The  $\text{pK}_{\text{a}}$  on the basic side of the D-malate  $V/K$  pH profile represents an enzymatic group, since neither tartrate nor malate has a  $\text{pK}$  value in this pH range. The lack of observation of the group in the  $V_{\text{malate}}$  pH profile suggests it is required to be protonated for optimal binding of the  $\beta$ -carboxylate of D-malate or tartrate. Consistent with this idea is the observation that the basic  $\text{pK}_{\text{a}}$  is present on the  $V/K_{\text{tartrate}}$  profile. TDH catalyzes the oxidation of (+)-tartrate to oxaloglycolate using NAD. Therefore, there is no obvious need for a catalytic acid in this reaction, but since a  $\text{pK}_{\text{a}}$  on the basic side of the  $V/K_{\text{tartrate}}$  profile is observed, this group is likely involved in binding tartrate. Since this interaction would be anticatalytic once the oxalacetate intermediate is formed, there must be rearrangement of bound oxalacetate in order to facilitate decarboxylation. The group may also participate in catalysis as a general acid donating a proton to enolpyruvate to form pyruvate as is the case in the oxidative decarboxylation of L-malate by malic enzyme (4, 5, 22).

**Possible Identity of Catalytic/Binding Groups.** The IPMDH from several species shares about 50% identity with the TDH from *P. putida* and has been proposed to be the evolutionary progenitor of TDH (10, 19). Of the 11 amino acid residues of the *Thermus thermophilus* IPMDH proposed to interact with IPM in the closed conformation (20), all but one is conserved in TDH. The exception is E87 in IPMDH that was proposed to interact with the isopropyl group of IPM. The homologous residue in TDH is a tryptophan. IPMDH has a lysine/tyrosine pair, K186 and Y139 in the *T. thermophilus* enzyme; a similar lysine/tyrosine pair has been implicated as important in the structure–function relationships of ICDH (21) and malic enzyme (22). In malic enzyme the lysine has been proposed to be the general acid. In TDH residues homologous to the IPMDH lysine/tyrosine pair are K192 and Y141. Consequently, K192 may be the group that must be protonated to bind the  $\beta$ -carboxylate in TDH and that may additionally serve as a general acid as proposed for K199 in the *Ascaris suum* NAD-malic enzyme reaction (22).

In IPMDH there are three aspartate residues in close vicinity to the bound  $\text{Mg}^{2+}$ . The homologous residues in TDH are D225, D250, and D254, and these residues may provide the primary coordination ligands to the divalent metal ion activator. Aspartate residues provide the ligands to the divalent metal ion activator in malic enzyme (24), and one of these has been proposed to be the general base (25). One of the homologous aspartate ligands to the divalent metal in TDH may also be the general base in TDH.

The NAD analogues thio-NAD, APAD, and PAAD are substrates for the TDH reaction (26). Thio-NAD has a  $V/E_t$

value very similar to NAD, but the  $K_m$  value for D-malate is increased about 10-fold compared to the value with NAD. Beecher et al. (26) have reported that the  $K_m$  values for D-malate were not significantly altered with the alternative dinucleotides. The reason for this discrepancy is unknown.

**Interpretation of Isotope Effects and Partition Ratios.** The theory of multiple isotope effects on enzyme-catalyzed reactions developed by Hermes et al. (2) allows one to distinguish between a concerted and a stepwise mechanism. Two isotope effects are measured,  $^{13}(V/K)_H$ , a  $^{13}\text{C}$  isotope effect using D-malate, and  $^{13}(V/K)_D$ , a  $^{13}\text{C}$  isotope effect using D-malate-2-*d*. If  $^{13}(V/K)_D$  is equal to or greater than  $^{13}(V/K)_H$ , data suggest a concerted reaction with respect to the two isotope effects. If  $^{13}(V/K)_D$  is less than  $^{13}(V/K)_H$ , data suggest the reaction is stepwise since substitution with deuterium will slow the hydride transfer step, a step separate from the  $^{13}\text{C}$  sensitive step of decarboxylation, and serve to partially mask the decarboxylation step. Qualitatively, the mechanism for TDH is stepwise with either NAD or thio-NAD since the  $^{13}\text{C}$  isotope effect decreases upon deuteration of D-malate. Hermes et al. (2) developed equations that should be satisfied for a stepwise mechanism where hydride transfer precedes decarboxylation.<sup>2</sup> In this case the equation is  $[^{13}(V/K)_H - 1]/[^{13}(V/K)_D - 1] = {}^D(V/K)/{}^D K_{eq}$ , where  ${}^D K_{eq}$  is equal to 1.18 (18). Substituting the average values of the isotope effects into the equation gives  $1.22 = 1.24$  for NAD and  $1.26 = 1.28$  for thio-NAD. The equation holds for both dinucleotide substrates and also suggests that the experimentally determined average values are well determined.

The  $^{13}\text{C}$  isotope effect data and the partitioning data may be used to calculate an estimate of the intrinsic  $^{13}\text{C}$  isotope effect ( $^{13}k$ ) using the equation  $^{13}k = ^{13}(V/K)_H + r_H[^{13}(V/K)_H - 1]$  or  $^{13}k = ^{13}(V/K)_D + r_D[^{13}(V/K)_D - 1]$  if the values with deuterium-labeled substrates are used (14). With NAD as the dinucleotide substrate the calculated intrinsic  $^{13}\text{C}$  isotope effect is 1.014 and 1.025 with protium- and deuterium-labeled substrates, respectively. There is fair agreement between the two values, suggesting the average, 1.02, is a good estimate for  $^{13}k$ . For thio-NAD the calculated values of  $^{13}k$  are 1.034 and 1.035, giving better agreement between the two calculated values of  $^{13}k$  than with NAD. The theoretical maximum value for a  $^{13}\text{C}$  primary kinetic isotope effect is about 6%, but values around 5% are obtained for the malic enzyme reaction (3, 6, 7). The relatively small values for the intrinsic  $^{13}\text{C}$  isotope effect in the TDH reaction suggest an early transition state for decarboxylation.

The partition ratio,  $r_H$ , is the ratio of the rate of decarboxylation to the rate of reduction of the OAA and was found to be pH dependent. The value of the pyruvate/malate ratio increases as the pH increases. The  $\text{p}K_a$  values on the partition ratios are similar to the  $\text{p}K_a$  observed on the acid side of the  $V/K$  profiles and likely represent the same enzymatic group, the general base. This would correspond well with the expected protonated form of the general base once hydride transfer has occurred. The pH dependence of the partition ratio results from OAA binding to enzyme when this group is either protonated or unprotonated, unlike the malic enzyme from *A. suum* where the partition ratio is pH independent as a result of OAA binding to only the protonated form of the

enzyme (26). For hydride transfer from the reduced dinucleotide to OAA to proceed, this group would need to be protonated, acting as a general acid, donating a proton to the carbonyl oxygen of OAA to assist hydride transfer. At higher pH values, where the general base is not fully protonated, decarboxylation could proceed regardless of the protonation state of the group, leading to higher partition ratios. Consequently, only at low pH where the group is fully protonated and hydride transfer can proceed at a maximum rate will the true partition ratio be observed. Substituting NADD or thio-NADD for the reduced protio dinucleotide substrate increases the pyruvate/malate ratio as expected since deuteration should decrease the rate of hydride transfer. Substituting thio-NADH for NADH leads to higher partition ratios since hydride transfer is thermodynamically less favorable with thio-NAD, and thus there is likely a higher energy barrier to hydride transfer with the less reducing dinucleotide.

**Comparison to Other Oxidative Decarboxylases.** Malic enzyme catalyzes the same oxidative decarboxylation reaction as does TDH, albeit with the L-isomer rather than the D-isomer. The intrinsic  $^{13}\text{C}$  isotope effect in the malic enzyme reaction is about 5–7% depending on the divalent metal ion used (7) and is similar to the average value of about 5% measured in solution (27). This observation suggests a similar late transition state for decarboxylation both in solution and in the malic enzyme reaction. It also suggests that in the malic enzyme-catalyzed reaction as in solution the OAA intermediate is directly coordinated to the divalent metal ion activator. Additional evidence for direct coordination of the substrate to the metal ion in the malic enzyme reaction comes from the observation that the inhibition constants for a series of malate analogues could be correlated with the metal–ligand dissociation constants. Also, the  $K_m$  for malate changes with the identity of the metal ion and is correlated with the metal–ligand dissociation constant (7). In contrast, in the TDH reaction the  $K_m$  for D-malate is unchanged when the metal ion is changed from Mg to Mn (1), suggesting the metal ion plays no significant role in binding substrate in TDH. In the IPMDH–IPM complex the crystal structure indicates that the  $\text{Mn}^{2+}$  activator is  $>4.0 \text{ \AA}$  from the isopropylmalate substrate, which is too great a distance for interactions between the two. If IPMDH is a good model for TDH, then D-malate likely also binds a significant distance from the divalent metal ion activator in an open conformation and could explain why there is no effect on the D-malate  $K_m$  value with metal ion. Fluorescence and slow-binding inhibition studies with oxalate (26) have indicated that there is a conformation change after TDH binding substrates. Closure of the active site on formation of the ternary IPMDH–NAD–IPM complex could bring the metal ion closer to the substrate to provide direct interactions between the metal and substrate. The ESEEM data on TDH of Tipton and Peisach (23) placed  $\text{Mn}^{2+}$  in close vicinity to substrate but could not determine if the metal was directly coordinated to D-malate. An outer sphere complex between malate and  $\text{Mn}^{2+}$  and by extension between  $\text{Mn}^{2+}$  and the OAA intermediate may account for some of the differences seen between malic enzyme and TDH. In malic enzyme the change from a stepwise to a concerted mechanism on changing the dinucleotide substrate from NAD to APAD or thio-NAD has been attributed to the OAA intermediate

<sup>2</sup> Application of Student's *t*-test indicates that the two values are significantly different at  $P = 0.5$ .

existing in a shallow energy well that collapses on changing to the more oxidizing dinucleotide substrate. The metal ion is thought to be involved in destabilizing the keto acid intermediate leading to the shallow energy well. If D-malate in the TDH reaction is in outer sphere complex with  $\text{Mn}^{2+}$ , the decarboxylation reaction could still be assisted by the divalent metal ion but may lead to a more stable OAA intermediate. Consequently, changing to a more oxidizing dinucleotide substrate would not result in a switch from a stepwise to a concerted mechanism as seen in the malic enzyme reaction. The metal ion in an outer sphere complex with OAA would be a less efficient Lewis acid than if directly coordinated to OAA where the metal could delocalize more of the electron density from the carbonyl oxygen and thus the C3–C4 bond of OAA. A greater degree of delocalization should lead to an earlier transition state, not later, as seen in malic enzyme. It seems more likely that other differences associated with the orientation of OAA in the active site and interactions with groups lining the active site are more important in determining the transition state structure of the decarboxylation reaction.

## REFERENCES

1. Tipton, P. A., and Peisach, J. (1990) *Biochemistry* 29, 1749–1756.
2. Hermes, J. D., Roeske, C. A., O'Leary, M. H., and Cleland, W. W. (1982) *Biochemistry* 21, 5106–5114.
3. Weiss, P. M., Gavva, S. R., Harris, B. G., Urbauer, J. C., Cleland, W. W., and Cook, P. F. (1991) *Biochemistry* 30, 5755–5763.
4. Schimerlik, M., and Cleland, W. W. (1977) *Biochemistry* 16, 576–583.
5. Kiick, D. M., Harris, B. G., and Cook, P. F. (1986) *Biochemistry* 16, 227–236.
6. Karsten, W. E., and Cook, P. F. (1994) *Biochemistry* 33, 2096–2103.
7. Karsten, W. E., Gavva, S. R., Park, S.-H., and Cook, P. F. (1995) *Biochemistry* 34, 3253–3260.
8. Edens, W. A., Urbauer, J. G., and Cleland, W. W. (1997) *Biochemistry* 36, 1141–1147.
9. Hwang, C.-C., Berdis, A. J., Karsten, W. E., Cleland, W. W., and Cook, P. F. (1998) *Biochemistry* 37, 12596–12602.
10. Tipton, P. H., and Beecher, B. S. (1994) *Arch. Biochem. Biophys.* 313, 15–21.
11. Tipton, P. H. (1993) *Biochemistry* 32, 282–2827.
12. O'Leary, M. H. (1980) *Methods Enzymol.* 64, 83–104.
13. Craig, N. (1957) *Geochim. Cosmochim. Acta* 12, 133–140.
14. Grissom, C. B., and Cleland, W. W. (1985) *Biochemistry* 24, 944–948.
15. Cleland, W. W. (1979) *Methods Enzymol.* 63, 103–108.
16. Northrop, D. B. (1977) in *Isotope Effects on Enzyme Catalyzed Reactions* (Cleland, W. W., O'Leary, M. H., and Northrop, D. B., Eds.) p 122, University Park Press, Baltimore, MD.
17. Cook, P. F., and Cleland, W. W. (1981) *Biochemistry* 20, 1790–1796.
18. Cook, P. F., Blanchard, J. S., and Cleland, W. W. (1980) *Biochemistry* 19, 4853–4858.
19. Tipton, P. A. (2000) *Protein Pept. Lett.* 7, 323–332.
20. Kadono, S., Sakurai, M., Moriyama, H., Sato, M., Hayashi, Y., Oshima, T., and Tanaka, N. (1995) *J. Biochem.* 118, 745–752.
21. Lee, M. E., Dyer, P. H., Klein, O. D., Bolduc, J. M., Stoddard, B. L., and Koshland, D. E. (1995) *Biochemistry* 34, 378–384.
22. Lui, D., Karsten, W. E., and Cook, P. F. (2000) *Biochemistry* 39, 11955–11960.
23. Tipton, P. A., and Peisach, J. (1991) *Biochemistry* 30, 739–744.
24. Xu, Y. W., Bhargava, G., Wu, H., Loeber, G., and Tong, L. (1999) *Structure* 7, 877–889.
25. Karsten, W. E., Chooback, L., Liu, D., Hwang, C.-C., Lynch, C., and Cook, P. F. (1999) *Biochemistry* 38, 10527–10532.
26. Park, S.-H., Harris, B. G., and Cook, P. F. (1986) *Biochemistry* 25, 3752–3759.
27. Grissom, C. B., and Cleland, W. W. (1986) *J. Am. Chem. Soc.* 108, 5582–5583.
28. Beecher, B. S., Koder, R. G., and Tipton, P. A. (1994) *Arch. Biochem. Biophys.* 315, 255–261.

BI026278G